Journal of Neuroimmunology 337 (2019) 577067

Contents lists available at ScienceDirect

Journal of Neuroimmunology

journal homepage: www.elsevier.com/locate/jneuroim

Dynamic expression of autophagy-related factors in autoimmune encephalomyelitis and exploration of curcumin therapy

Yuan Boyao[a,1], Sun Mengjiao[a,1], Bao Caicai[a], Li Xiaoling[a], Liu zhenxing[b], Wang Manxia[a,*]

[a] Neurology Department, Second Hospital of Lanzhou University, Lanzhou, Gansu 730030, China
[b] Department of Gastrointestinal Surgery, Affiliated Hospital of Zunyi Medical College, Zunyi, Guizhou 563003, China

ARTICLE INFO

Keywords:
Multiple sclerosis
Experimental autoimmune encephalomyelitis (EAE)
Curcumin
Autophagy
mTOR

ABSTRACT

Curcumin has been used in the study of central nervous system immune-related diseases and exerts a substantial neuroprotective effect. However, the mechanism remains unclear. The AKT/mTOR autophagy-related signalling pathway plays an important role in tumour therapy, but whether curcumin plays a therapeutic role in multiple sclerosis (MS) through this signalling pathway remains to be determined. As an animal model of MS, experimental autoimmune encephalomyelitis (EAE) is induced by the myelin glial glycoprotein MOG35-55 in female C57BL/6 mice. We first evaluated the changes in autophagy levels in EAE mice. Then, curcumin was intraperitoneally injected into the mice, and the expression of AKT/mTOR autophagy signalling pathway-related proteins was evaluated. Our data show that 1. autophagy defects can cause neuronal damage in EAE mice; and 2. curcumin may regulate the activation of autophagy in EAE mice by affecting the AKT/mTOR autophagy signalling pathway, further balancing central nervous system and peripheral autophagy.

1. Introduction

As a common central nervous system (CNS) inflammatory demyelinating disease, multiple sclerosis (MS) currently affects approximately 2.5 million people worldwide, mainly among young people and females (Dendrou and Fugger, 2017). The disease is characterized by inflammatory demyelination and neuronal degeneration, and patients are often affected by varying degrees of neurological symptoms. Long-term progress can lead to the accumulation of CNS lesions and even the occurrence of various complications of disability, seriously affecting patient health (Hemmer et al., 2015).

The pathogenesis of MS is still unclear. In recent years, some scholars have discovered that autophagy is involved in the pathophysiological process of nervous system immune diseases and degenerative diseases (Tian et al., 2011). Autophagy is a non-invasive response of cells to sustained internal and external stimuli that maintains cell structure, metabolism and homeostasis. It can be divided into macroautophagy, microautophagy and molecular chaperone-mediated autophagy according to the way the substrate enters the lysosome, and the most widely studied form is macroautophagy (Zhang, 2015). Studies have reported that autophagy not only plays an important role in maintaining the normal physiological function of cells but also participates in the body's immune response under pathological conditions. There is a dual regulation of the immune response in CNS disease, which may affect the occurrence, development and outcome of MS (Schmid et al., 2007). In studies on experimental autoimmune encephalomyelitis (EAE, an animal model of MS), autophagy defects were found to lead to EAE-induced neuronal damage, and the use of autophagy-regulating drugs could alter inflammatory infiltration, clinical scores, and the degree of neuronal damage (Feng et al., 2017). Therefore, in recent years, research on the role of autophagy in the pathogenesis and treatment of MS has attracted attention, and the regulation of autophagy has become a promising new therapeutic concept. For MS treatment, although > 10 disease-modifying drugs are available for clinical use, most MS patients still have varying degrees of disability and persistent clinical symptoms. Therefore, it is important to further explore drugs for MS treatment. There have been many studies on the prevention and treatment of MS by plant extracts from natural compounds at home and abroad. Curcumin has shown neuroprotective effects in MS and the EAE model (Mohajeri et al., 2015). Some scholars have reported that in EAE mice, curcumin shortens the clinical course and reduces the proportion of TH17 cells and the levels of chemotactic cytokines (Kanakasabai et al., 2012). Studies have also shown that curcumin significantly reduces the number of apoptotic cells and inhibits the upregulation of cyt-c, caspase-9 and caspase-3 in EAE mice, suggesting that curcumin can inhibit apoptosis in EAE mice. This

* Corresponding author at: Second Hospital of Lanzhou University, No. 82, Cuiyingmen, Chengguan District, Lanzhou City, Gansu Province, China.
E-mail address: wmx322@aliyun.com (W. Manxia).
[1] Yuan Yaobo and Sun Meng jiao are the co-first authors. They contributed equally to the manuscript.

https://doi.org/10.1016/j.jneuroim.2019.577067
Received 28 October 2018; Received in revised form 17 February 2019; Accepted 10 September 2019

compound may act by preventing mitochondrial damage and inhibiting the intrinsic apoptotic pathway (Feng et al., 2014). Some scholars have also found that the application of polymeric nano-curcumin (PNC), an anti-inflammatory and anti-oxidative stress agent, has a significant effect in the rat EAE model and impacts EAE scores and myelin repair (Mohajeri et al., 2015). Recent studies have shown that in tumour cells, curcumin can play a role by affecting the protein kinase B/mammalian rapamycin target protein (AKT/mTOR) signal transduction pathway, which is important in autophagy (Wei et al., 2017). However, there is still a lack of research on the specific mechanism of action of curcumin in MS or the EAE model. Therefore, this study establishes the EAE model to explore whether curcumin can exert its neuroprotective effect by affecting the AKT/mTOR autophagy signalling pathway and provides a theoretical basis for the identification of new effective drugs for MS.

2. Materials and methods

2.1. Mice

Female C57BL/6 mice (aged 6–8 weeks, weighing 18–20 g) were purchased from the Animal Experimental Center of Gansu University of Chinese Medicine in Gansu, China. The mice were maintained under specific pathogen-free conditions at room temperature (24 ± 2 °C) with a 12-h light/dark alternate cycle and were given free access to food and water. All animal experiments performed in this study were approved by the Institutional Animal Care and Use Committee of Lanzhou University and the local experimental ethics committee.

2.2. EAE induction and evaluation

The mice were randomly distributed to the control group, the EAE group, the rapamycin treatment group and the curcumin treatment group. The EAE group was divided into four subgroups: the pre-immune group (7 days), the pre-morbid group (14 days), the peak incidence group (21 days) and the disease recovery group (30 days). EAE was induced in the mice with a subcutaneous injection of 250 μg of the myelin oligodendrocyte glycoprotein (MOG) p35-55 peptide (CS Bio CS0681), as previously described. All peptides were dissolved in complete Freund's adjuvant (CFA; Sigma, MO, USA) containing 4 mg/ml heat-killed *Mycobacterium tuberculosis* H37Ra (Difco Laboratories, Detroit, MI, USA) (Li et al., 2012). On the day of immunization and 2 days later, the mice received an intraperitoneal (IP) injection of 500 ng of pertussis toxin (Alexis, San Diego, CA, USA). Clinical scores were measured daily, as follows: 0 - no paralysis; 1 - loss of tail tone; 2 - hindlimb weakness; 3 - hindlimb paralysis; 4 - severe hindlimb and forelimb paralysis; and 5 - moribund or death.

2.3. Rapamycin and curcumin treatment

The mice were separated randomly into a control group (n = 15), an EAE group (n = 30), an EAE-DMSO group (EAE mice treated with DMSO; n = 15), an EAE-Rapa group (EAE mice treated with rapamycin; n = 15), and an EAE-Cur group (EAE mice treated with curcumin; n = 15). Rapamycin (2 mg/kg; Sigma) or curcumin (10 mg/kg; Sigma) IP injections were given once daily for 15 days starting on the 8th day of EAE induction. EAE-DMSO mice received a daily IP injection of the same volume (0.2 ml /s; Sigma) of 20% DMSO solution.

2.4. Histological evaluation

The spinal cords were removed from the mice in each group 21 days post immunization. After anaesthetizing the mice with 10% chloral hydrate (0.2ml /mouse), 4% paraformaldehyde was perfused for 0.5 h. Then, the lumbar enlargement of the spinal cord was dissected, fixed and embedded in paraffin for pathological sectioning. The spinal cords were sliced into 5-μm-thick axial sections. These sections were stained with haematoxylin-eosin (H&E), Weil's stain and blue-cresyl violet to assess demyelination and inflammatory lesions (Zhen et al., 2015).

Histopathological findings were determined: The spinal cord sections stained by HE and WEIL were observed under an optical microscope. 3 spinal cord sections were taken from each mice, and 5 high-power (400 x) fields were selected for each spinal cord section for inflammatory infiltration and myelin loss score, and the mean inflammatory infiltration and myelin loss score were calculated for each mice.

H&E staining inflammation scoring criteria:

0 points: no inflammatory changes;

1point:inflammatory cell infiltration was only limited to the blood vessels and the spinal membrane;

2 points: mild inflammatory cell infiltration in the spinal cord, namely 1–10 pieces;

3 points: moderate inflammatory cell infiltration in the spinal cord, namely 11–100 pieces;

4 points: severe inflammatory cell infiltration in the spinal cord, namely > 100 tablets.

WEIL's criteria for scoring myelin sheaths:

0 points: white matter of normal brain or spinal cord;

1 point: point demyelination;

2 points: lamellar demyelination;

3 points: extensive demyelination involving the spinal cord.

2.5. Immunohistochemistry

Spinal cord sections were subjected to antigen retrieval using a microwave in 0.01 mol/L citrate solution for 15 min, then incubated with 3% H_2O_2 and blocked with goat serum at room temperature for 15 min; an anti-LC3-II antibody (1:200), anti-AKT antibody (1:200), anti-mTOR antibody (1:200) or anti-Beclin 1 antibody (1:100) was then added and incubated overnight at 4 °C. The sections were then incubated with a streptavidin-biotin-peroxidase complex (SABC) kit for 30 min, stained with 3,3′-diaminobenzidine (DAB), and counterstained with H&E. The mounted sections were sealed with epoxy resin, and the results were observed under a light microscope (Shen et al., 2016).

2.6. Western blot (WB) analysis

The total protein content of the spinal cords was extracted, subjected to sodium dodecyl sulfate-polyacrylamide gel electrophoresis and transferred to nitrocellulose membranes. The membranes were blocked in 5% (v/v) skim milk for 2 h at room temperature and then incubated overnight at 4 °C in primary antibody solution. Following 4 washes with 0.1% Tween in PBS, the membranes were incubated with the horseradish peroxidase-conjugated secondary antibody for 2 h at room temperature. The membranes were washed again to remove the unbound antibodies and detected by a WB detection system. The following antibodies were used: anti-Beclin 1 (1:1000, CST), anti-LC3-II (1:1000, CST), anti-p62 (1:500, CST), anti-AKT (1:1000, CST), anti-mTOR (1:500, CST), anti-p-AKT (1:200, CST), anti-p-mTOR (1:500, CST), and secondary antibody (1:1000, Santa Cruz Biotechnology). Positive signals were developed by an EasyBlot ECL Kit (Sangon Biotech, Shanghai, China) and analysed with ImageJ 1.49 (National Institutes of Health, Bethesda, MD, USA).

2.7. Real-time RT-PCR

For reverse transcriptase-polymerase chain reaction (RT-PCR) studies, the lumbar spinal cord was rapidly removed from the mice, immediately frozen in liquid nitrogen and stored until needed. Total RNA was extracted from the tissues using the total RNA isolation solution according to the manufacturer's guidelines. The yield of RNA was determined using a NanoDrop spectrophotometer (Thermo Fisher

Scientific Inc., MA, USA), and 1 μg of RNA was used for the synthesis of complementary DNA and subsequent PCR. Real-time PCR was performed using 5× HOT FIRPOL® EvAGreen qPCR Mix Plus (Solis BioDyne, Tartu, Estonia) and the CFX96TM Real-time Detection System (Bio-Rad Laboratories, CA, USA). The following primers were used for amplification: β-ACTIN forward: 5′-ATGCTCCCCGGGCTGTAT-3′ and β-ACTIN reverse: 5′-CATAGGAGTCCTTCTGACCCATTC-3′. Semi-quantitative analysis was performed by monitoring the real-time increase in the fluorescence of the EvAGreen dye on an i-Cycler (Bio-Rad Laboratories, CA, USA). To confirm single-band production, we performed a melt-curve analysis and confirmed the results by electrophoresis and Red Safe staining (iNtRON Biotechnology, Kyungki-Do, Korea). All data were normalized against actin mRNA levels and expressed as fold increases relative to controls.

2.8. ELISA

Twenty-one days after induction of the EAE model in the mice, 6 mice in each group were randomly selected for cardiac blood collection in heparin anticoagulation tubes. After centrifugation at 3000 r/min for 30 min, the upper plasma layer was collected and diluted at an appropriate ratio, and the mass concentrations of soluble IFN-γ, IL-17 and TNF-α were measured in strict accordance with the ELISA kit (Neobioscience, Shanghai, China) product specifications (Bravo et al., 2016).

2.9. Statistical analysis

Data are presented as the mean ± standard deviation. Statistical analyses of comparisons between two groups were performed by Student's *t*-test, while differences between three or more groups were analysed by one-way analysis of variance followed by the Newman-Keuls multiple comparison test. The data were analysed using SPSS 22.0 software (SPSS Inc., Chicago, IL, USA). A value of $p < .05$ was considered statistically significant.

3. Results

3.1. Dynamic expression of autophagy-related factors in the spinal cords of EAE mice

LC3-II is closely associated with the number of autophagosomes, and Beclin 1 is well known as an autophagy-related gene. p62 (SQSTM1/sequestosome 1) binds to LC3-II and can thus be used as an indicator of autophagic flux. The suppression of LC3-II, Beclin 1 and p62 expression reflects impaired autophagy (Kabeya et al., 2000). First, immunohistochemical staining was used to localize the expression of autophagy-related proteins in different stages of the EAE model. LC3-II and Beclin 1 were observed under a light microscope, and positive expression was visible as a brownish yellow colour (Fig. 1). Second, WB analysis was performed to monitor the levels of LC3-II, Beclin 1 and p62 in the spinal cords of mice on the 7th, 14th, 21st, and 30th days of EAE. Downregulation of LC3-II was observed in EAE mice compared with the control group at each time point, and the levels of LC3-II rebounded during the recovery period (30th day) (Fig. 2A and B). The level of Beclin 1 was also downregulated in EAE mice compared with that in the control group, but it returned to the control level on the 30th day (Fig. 2A and C). The expression of p62 was upregulated in the EAE group compared with the that in the control group at each time point (Fig. 2A and D). Overall, LC3-II and Beclin 1 showed a downward trend in EAE mice, reaching a minimum at the peak of the disease ($p < .05$) and slowly returning to the level of the control group after entering the chronic phase; the changes in p62 levels showed the opposite trend.

3.2. Influence of rapamycin and curcumin on pathological changes and clinical scores in EAE mice

To investigate the detailed functions of autophagy in EAE mice, histological evaluation was conducted in rapamycin- and curcumin-treated EAE mice using H&E and Weil staining. We found that both the population of infiltrated inflammatory cells and the area of the demyelinated lesion were smaller in EAE-rapamycin mice and EAE-curcumin mice compared to those of the EAE group (Fig. 3). However, there was no significant difference between EAE-rapamycin mice and EAE-curcumin mice.

In addition, compared with the EAE-vehicle group, the EAE-Rapa group and the EAE-curcumin group showed an obviously postponed onset of disease symptoms, a reduced disease incidence, and an improved clinical score. The mean symptom score and the highest symptom scores of the curcumin group and the rapamycin group were significantly different ($p < .05$) from those of the EAE group, but there was no significant difference between the two drug treatment groups. Overall, we inferred that autophagy recovery might ameliorate inflammation and demyelination and improve clinical scores in EAE mice (Fig. 4).

3.3. Influence of rapamycin and curcumin on AKT/mTOR autophagy signalling pathway-related factors in EAE mice

First, the spinal cord lumbar enlargement of the mice in each group at the peak of onset (21 days) was immunohistochemically stained. Positive expression of AKT, mTOR and LC3-II was visualised as a brownish yellow colour under light microscopy. The immunoreactive product of the AKT protein is mainly expressed in the cytoplasm, and a small amount is expressed on the cell and nuclear membranes. Positive expression in the spinal cord was observed in the control group. The expression in the EAE group and the DMSO group was significantly stronger than that in the normal group, while the expression in the curcumin group and the rapamycin group was not significantly stronger than that in the control group. The mTOR protein was mainly stained in the cytosol and membrane, and the control group also showed positive expression; the changes in mTOR were similar to the changes in AKT in each group. In contrast, LC3-II was expressed in the cytoplasm. Positive expression was observed in the spinal cord of the control group. The expression in the EAE group and the DMSO group was significantly weaker than that in the normal group, while the expression in the curcumin group and the rapamycin group was not significantly weaker than that in the control group (Fig. 5). In addition, WB analysis was used to study the regulation of the AKT/mTOR autophagy-related signalling pathway in spinal cord tissue 21 days after mouse EAE induction. WB detection of the phosphorylation state of AKT/mTOR is important because the activation of the signalling pathway is mediated by the phosphorylation of the proteins. Specifically, compared with the control group, p-AKT, p-mTOR and p62 were highly expressed in the spinal cord tissue of the EAE group, while LC3-II and Beclin 1 were expressed at low levels. In contrast, compared with the EAE group, p-AKT, p-mTOR, and p62 were downregulated in the curcumin group and rapamycin group, while LC3-II and Beclin 1 expression increased significantly (except p-AKT, $p < .05$); in addition, there was no significant difference between the two drug treatment groups ($p > .05$). There were no significant differences in the non-phosphorylated AKT and mTOR proteins between the EAE group and the curcumin group (Fig. 6).

3.4. Influence of rapamycin and curcumin on the expression of ATG5 and LC3-II mRNA in EAE mice

We investigated the expression of ATG5 and LC3-II mRNA in the spinal cords of mice in the EAE model of MS by real-time RT-PCR. ATG5 expression was decreased in the EAE group compared to that of the

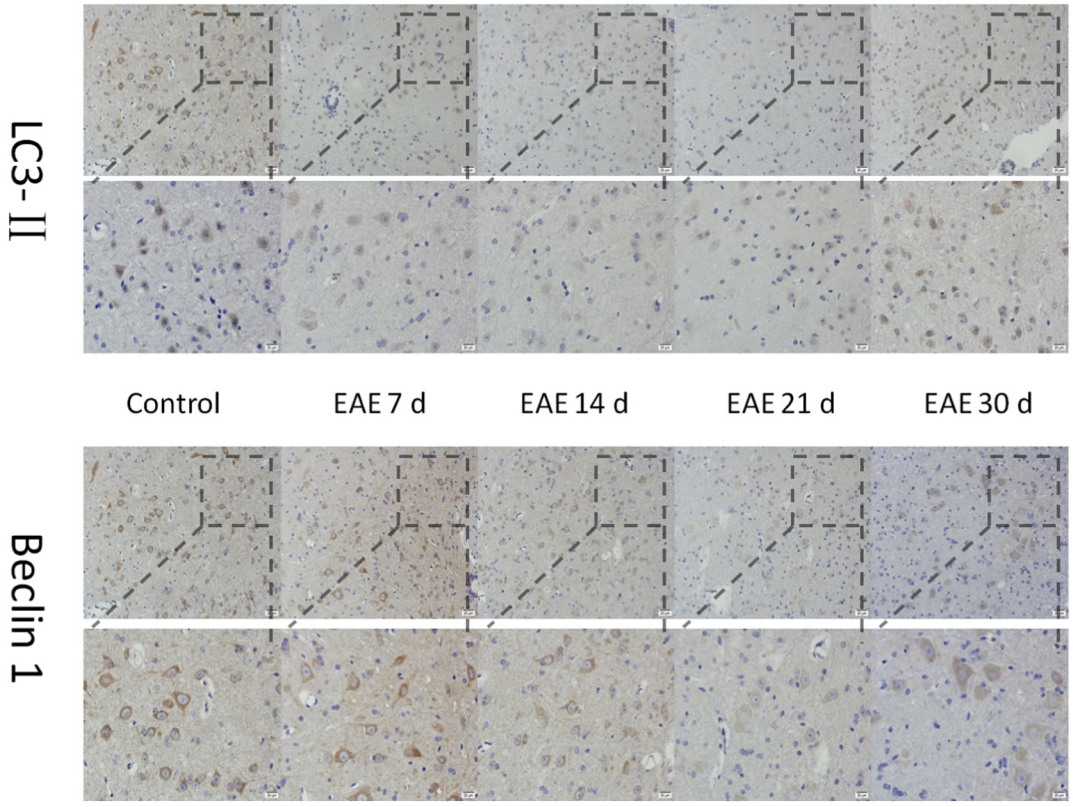

Fig. 1. Immunohistochemical images of LC3-II and Beclin 1 in the spinal cord (200× and 400×).

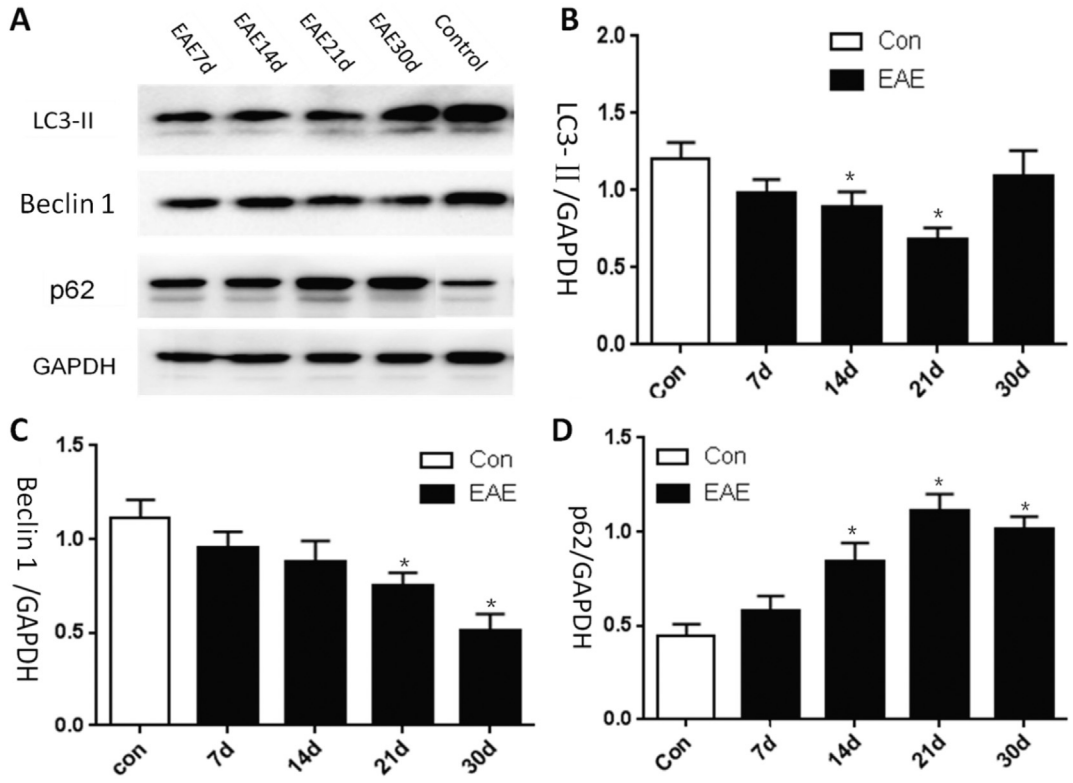

Fig. 2. Expression of the LC3-II, Beclin 1 and p62 proteins detected by Western blotting in the spinal cord at various time points. A and B show a WB analysis of LC3-II protein levels in the spinal cord of EAE mice on days 7, 14, 21 and 30 after EAE induction. A and C show a WB analysis of Beclin 1 protein levels at 7, 14, 21 and 30 days post immunization. A and D show a WB analysis of p62 protein levels at 7, 14, 21 and 30 days post immunization. Three spinal cord samples were tested at each time point, and * indicates that the difference was statistically significant, with $p < .05$ compared with the control group.

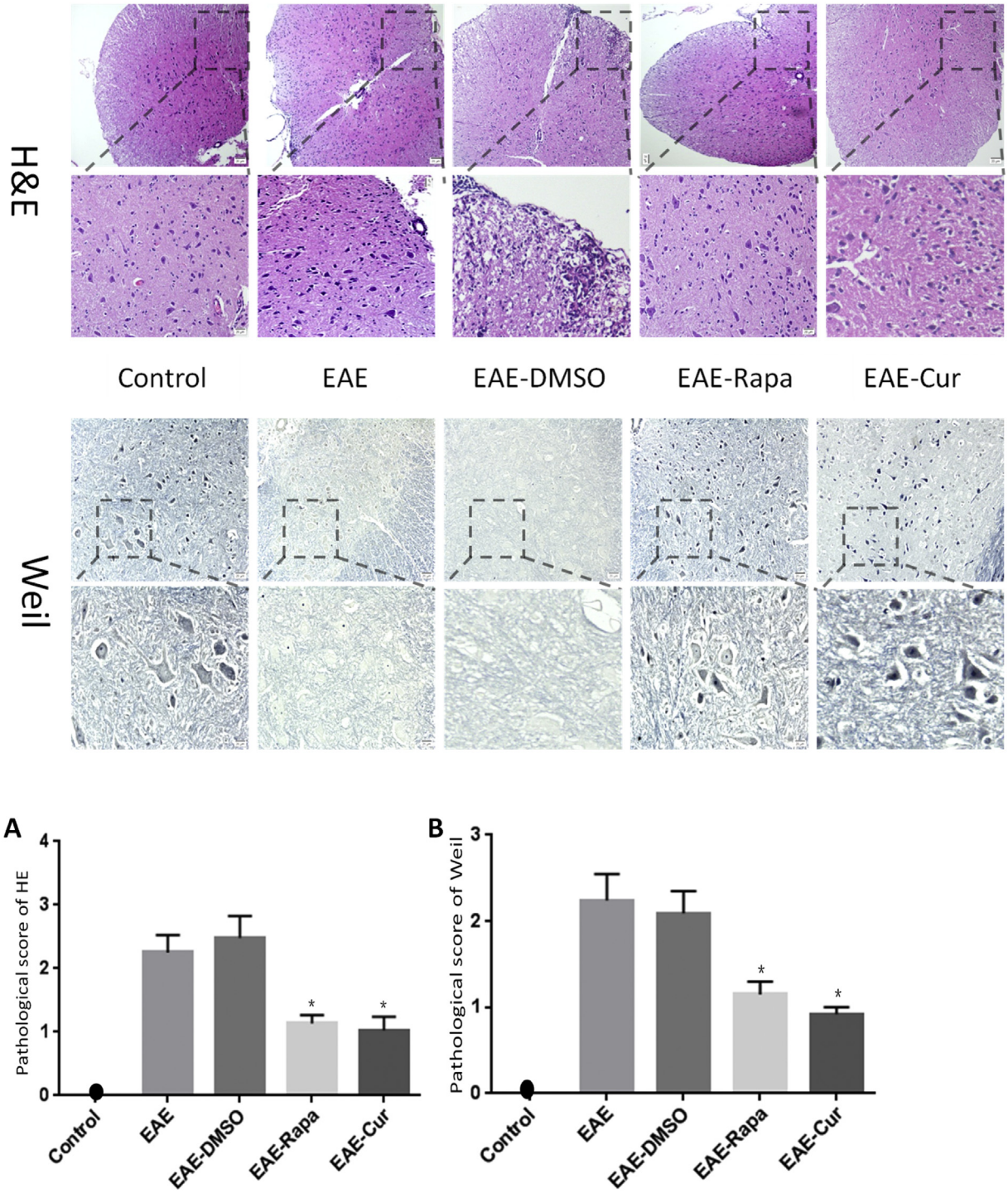

Fig. 3. Infiltration of inflammatory cells detected by H&E staining (40× and 200×) and myelin loss detected by Weil staining (200× and 400×) in spinal cord tissue. The lumbar spinal cords were sampled on the 21st day after experimental autoimmune encephalomyelitis (EAE) induction from the control, EAE, EAE-DMSO, EAE-rapamycin (Rapa) and EAE-curcumin (Cur) groups. The tissues were subjected to paraffin sectioning and stained with H&E and Weil's stain. Quantification of (A) infiltrated inflammatory cells and (B) the demyelinated lesion area. * indicates that the difference was statistically significant, with $p < .05$ compared with the EAE group.

control group. Rapamycin and curcumin administration were able to increase the level of ATG5 expression ($p < .05$; Fig. 7A). We observed that in the EAE-Rapa group and the EAE-Cur group, ATG5 expression was increased compared to that of the MOG-induced EAE group ($p < .05$; Fig. 7B). Similarly, the trend of LC3-II was similar to that of ATG5, and we observed that LC3-II expression was also decreased in the EAE group compared to that of the control group. In the EAE-Rapa group and the EAE-Cur group, LC3-II expression was increased compared to that of the MOG-induced EAE group ($p < .05$). There were significant differences in the expression of ATG5 and LC3-II between the two drug treatment groups ($p < .05$).

3.5. Influence of rapamycin and curcumin on inflammatory factors in EAE mice

On the 21st day after model establishment, peripheral blood was

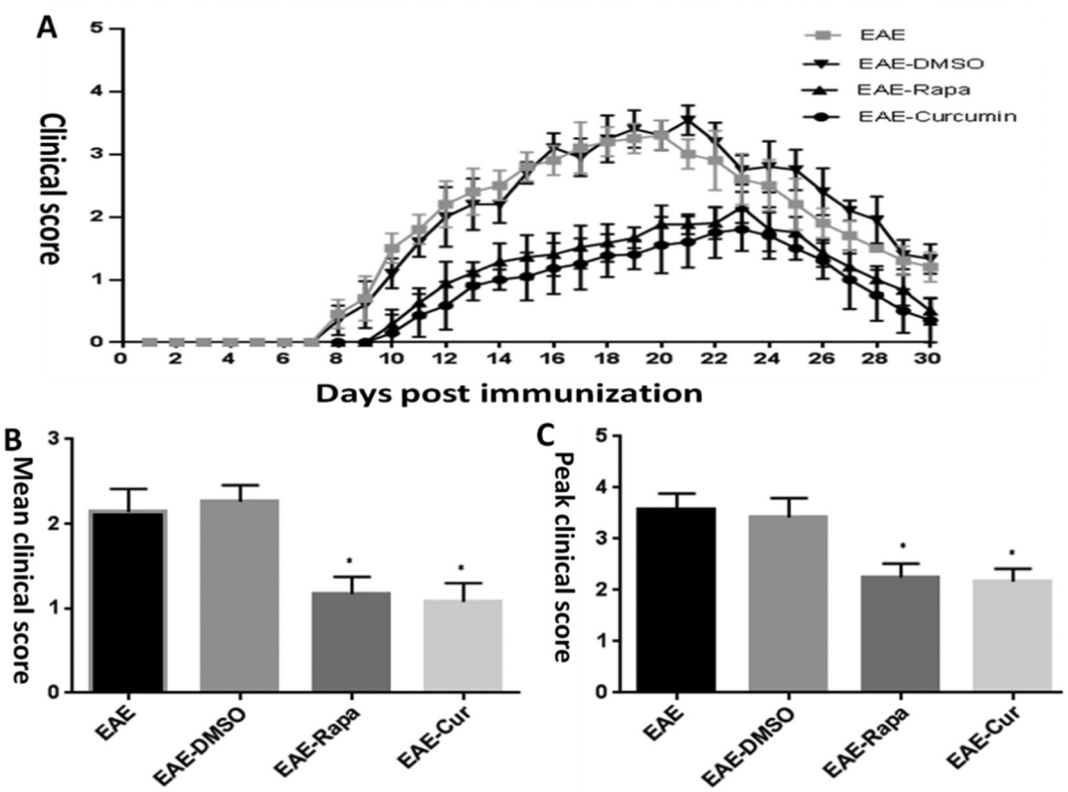

Fig. 4. Symptom scoring of mice after immunization (A) Comparison of the clinical scores of the EAE group, the DMSO group, the rapamycin group, and the curcumin group. For clinical scores, $n = 6$ mice per group. (B) and (C) Bar graphs of the mean clinical symptom scores and highest symptom scores for each group of mice. * indicates that the difference was statistically significant, with $p < .05$ compared with the EAE group.

collected from each group of mice. The concentrations of soluble IFN-γ, IL-17 and TNF-α in the plasma were detected by ELISA. The results showed that the expression of IFN-γ, IL-17 and TNF-α in the EAE mice was significantly higher than that in the normal group ($p < .05$), while the concentrations of IFN-γ and IL-17 in the curcumin-treated and rapamycin-treated mice were significantly lower than those of the EAE model ($p < .05$). Compared with those of the rapamycin group, the expression levels of IL-17 and IFN-γ in the curcumin treatment group decreased slightly; in contrast, the TNF-α level increased, but the difference was not significant ($p > .05$) (Fig. 8).

4. Discussion

Autophagy is a lysosome-dependent degradation pathway that is

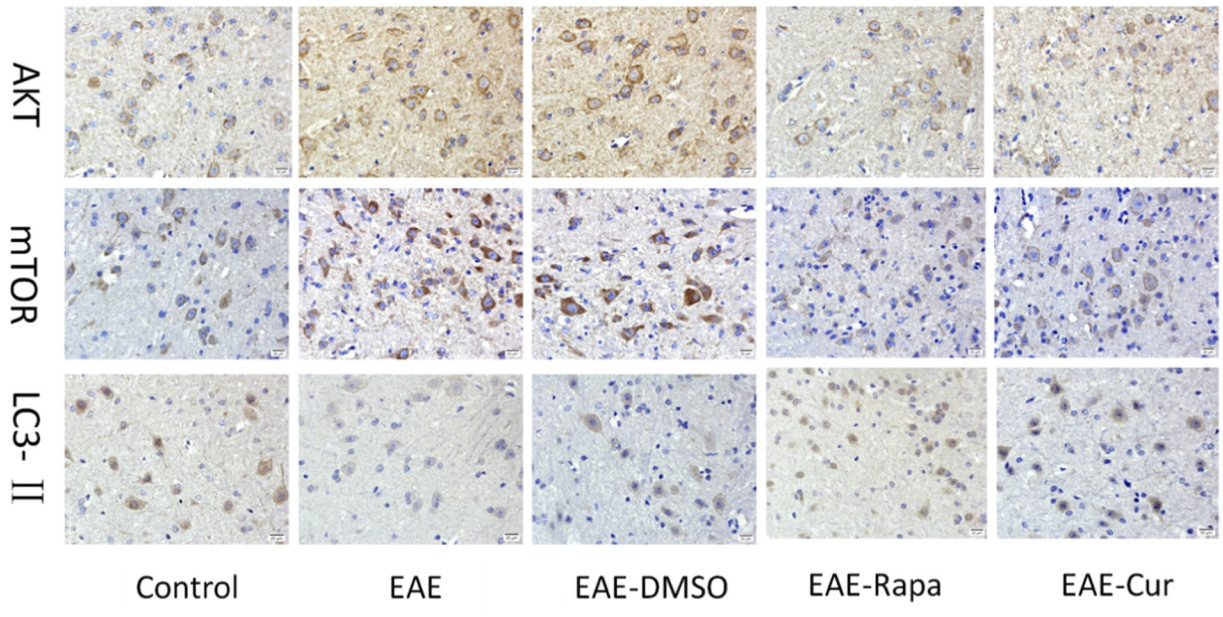

Fig. 5. Immunohistochemical images of AKT, mTOR, and LC3-II in the spinal cord (400×).

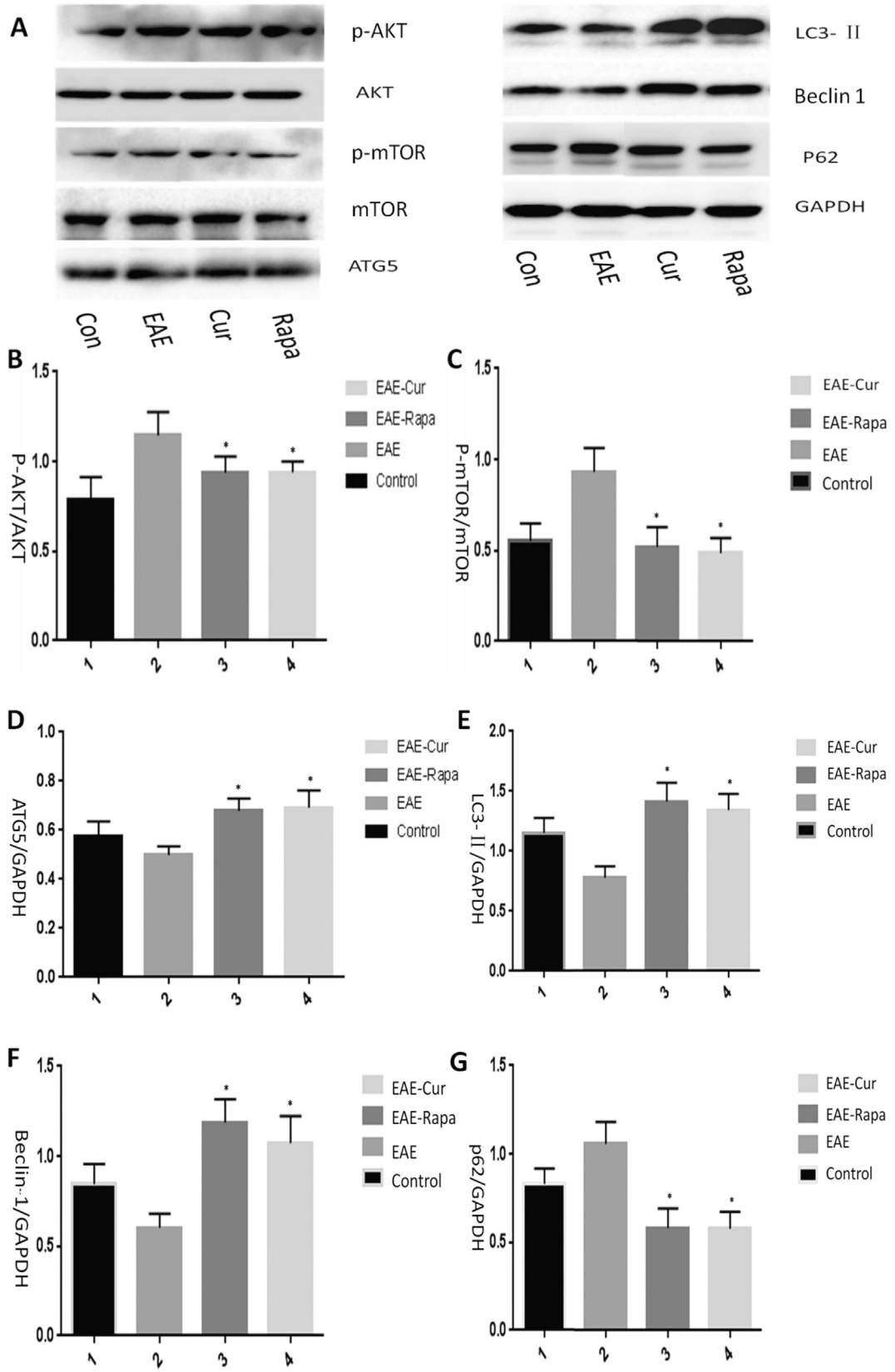

Fig. 6. Expression of the p-AKT, AKT, p-mTOR, mTOR, ATG5, LC3-II, Beclin 1 and p62 proteins detected by Western blotting in the spinal cord in individual groups. (A) WB analysis of p-AKT, AKT, p-mTOR, mTOR, ATG5, Beclin 1, LC3-II and p62 in the spinal cord in the control group, EAE group, rapamycin group and curcumin group. (B) and (C) Histograms of the spinal p-AKT/AKT and p-mTOR/mTOR proteins in each group. (D), (E), (F), (G) Quantification of ATG5, LC3-II, Beclin 1 and p62 protein expression in the spinal cord of each group. Three spinal cord samples were tested in each group, and * indicates $p < .05$ compared with the EAE group. The difference was statistically significant.

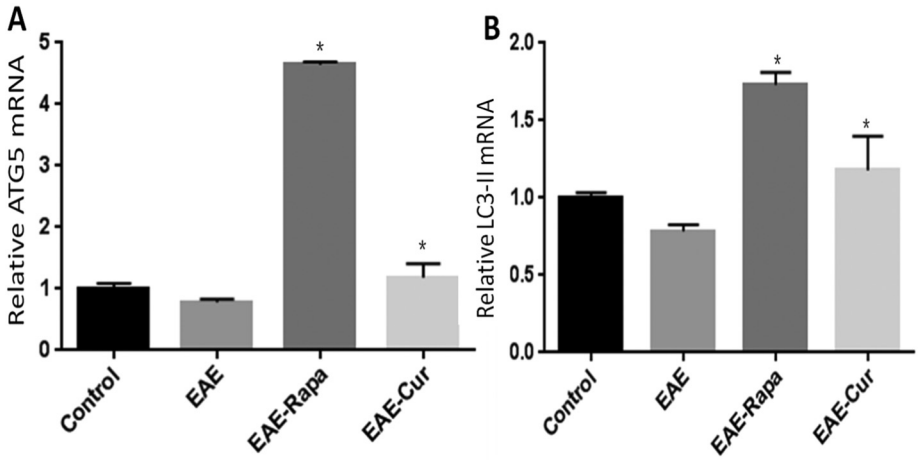

Fig. 7. The expression of ATG5 and LC3-II mRNA in the spinal cords of mice in the EAE model of MS by real-time RT-PCR. (A) and (B) Relative expression of ATG5 and LC3-II mRNA in the spinal cord of each group. Three spinal cord samples were tested in each group, and * indicates $p < .05$ compared with the EAE group. The difference was statistically significant.

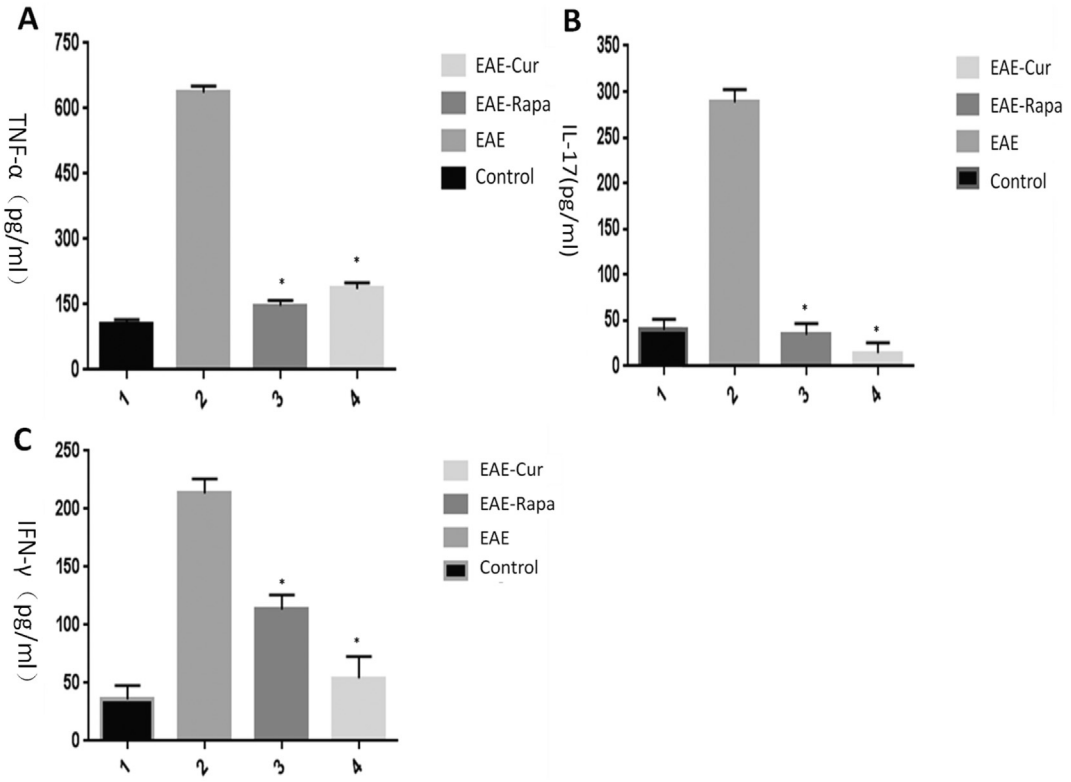

Fig. 8. ELISA results for cytokine concentrations in the peripheral blood of all groups. (A), (B), and (C) Bar graphs showing the concentrations of IFN-γ, IL-17, and TNF-α in the peripheral blood of the mice in each group by ELISA. Three spinal cord samples were tested in each group, and * indicates $p < .05$ compared with the EAE group. The difference was statistically significant.

triggered by a variety of internal and external stimuli and involves a series of complex processes that ultimately degrade unwanted organelles and proteins into amino acids that can be used for energy cycling (Patergnani et al., 2018). The autophagy process mainly consists of five stages. Initially, the formation of a bilayer membrane structure (initial/nucleation stage) from different organelles begins in the cytoplasm. Then, the membrane gradually diffuses (elongation phase), and with the fusion of the edge of the membrane, the protein that needs to be degraded is encapsulated to form autophagosomes (mature stage). The autophagosomes fuse with lysosomes to form autophagosomes (fusion phase), and finally, lysosomal enzymes digest the intravesicular material (degradation period) (Liang and Le, 2015). Various biomolecules participate in different stages of autophagy and gradually dissociate after the autophagy process is completed (Orrenius et al., 2013). Among these molecules, Beclin 1 is a key component of the Beclin 1/VPS34/VPS15/Atg14 complex that is involved in autophagosome formation and maturation. LC3-II is a specific protein that is present on the autophagosome membrane, and the autophagy level is closely related to the number of autophagosomes. Moreover, autophagosomes recognize the degradant through binding to the LC3-II domain via the adaptor protein p62. Therefore, the expression of LC3-II, Beclin 1 and p62 reflects the level of autophagy in the body (Wu and Adamopoulos, 2017; Zhen et al., 2015). In addition, studies have found that LC3-II expression is decreased, and autophagy flux is impaired in EAE mice, which may be due to decreased autophagosome formation and increased autophagocytic degradation (Boland and Nixon, 2006).

In recent years, pharmacological regulation of autophagy has been recognized as a potential treatment for the prevention or treatment of neurodegenerative diseases. Therefore, it is important to explore autophagy-related signalling pathways in MS and EAE and investigate

their potential mechanisms of action.

Curcumin is a hydrophobic polyphenol derived from herbaceous turmeric, which is derived from the rhizome of turmeric. Curcumin exerts its beneficial effects through anti-oxidative, anti-proliferative and anti-inflammatory properties and is commonly used in traditional medicine to treat inflammation and promote wound healing. In recent years, curcumin has been gradually used as an auxiliary drug for various diseases, such as cancer, arthritis, and immune diseases (Evans et al., 2018). Studies have shown that in the spinal cord injury (SCI) animal model, curcumin can improve the severity of symptoms in the SCI model by regulating the mTOR signalling pathway (Lin et al., 2017). In addition, a small clinical study included 80 patients with relapsing-remitting MS (RRMS) who were treated with the small molecule curcumin as an adjunct to IFN-β1a, but the results have not been published (Ledinek et al., 2013). In research reports on MS and EAE models, curcumin plays an important role in anti-inflammatory effects, improving clinical conditions and protecting neurons. Based on these reports, we attempted to use curcumin for treatment in the mouse EAE model.

The AKT/mTOR pathway is an intracellular signalling pathway that regulates cell activation, proliferation, metabolism, and apoptosis. AKT plays an important role in cell survival and apoptosis and is involved in cellular processes, including apoptosis and glucose metabolism. mTOR is a phosphorylated protein substrate of the serine/threonine phosphatidylinositol 3-kinase-associated kinase (PIKK) family (Hubbard et al., 2014) and is composed of two homologous complexes, mTORC1 and mTORC2, of which mTORC1 is resistant to rapamycin. mTOR has high sensitivity and plays an important role in the regulation of autophagy. mTOR is a downstream effector of AKT, and phosphorylated AKT can indirectly activate the key regulator of mTORC1 during the initiation phase of autophagy, which can inhibit autophagy after activation (Chen et al., 2015). Therefore, the mTORC inhibitor rapamycin is often used as an inducer of autophagy in clinical settings. In the AKT/mTOR pathway, activated PI3K produces the second messenger PIP3 on the plasma membrane, and activated PIP3 binds to the intracellular signalling proteins 3-phosphoinositide-dependent protein kinase 1 (PDK1) and AKT to recruit downstream PDK1 to the plasma membrane, which causes PDK1 to phosphorylate AKT, thereby activating AKT. When AKT is activated, it inhibits the formation of the TSC-1/TSC-2 complex, indirectly activating mTOR. Activated mTOR further phosphorylates two downstream molecules: the translation inhibitory molecule eIF-4E binding protein 1 (4E-BP1) and the ribosomal protein p70S6K. The phosphorylation of p70S6K activates its function and promotes protein synthesis, and these effects are inactivated after the phosphorylation of 4E-BP1, which initiates translation of the protein. Rapamycin inhibits the phosphorylation of p70S6K and downstream 4E-BP1, thereby inducing autophagy (Chi et al., 2015). The above events represent the general process of PI3K/AKT/mTOR pathway regulation. Studies have shown that autophagy has a close relationship with the AKT/mTOR pathway in MS. Exploring the relationship between the AKT/mTOR pathway and autophagy has important clinical value for applications in MS prevention and treatment (Kumar et al., 2013).

In the present study, we first found that the autophagy markers LC3-II and Beclin 1 gradually decreased in EAE mice with the progression of the disease and reached a minimum at the peak of the disease; the opposite changes were observed for p62. Moreover, this downregulation was restored after the application of an autophagy inducer, which significantly reduced the degree of inflammatory infiltration and demyelination in EAE mice, and the clinical score was also greatly improved. Second, based on the anti-inflammatory effects of curcumin, we localized the expression of AKT, mTOR and LC3-II in the spinal cord and quantitated the expression of AKT-mTOR autophagy-related proteins in the spinal cord. In addition, the expression of soluble IFN-γ, IL-17, TNF-α and other cytokines was detected in the peripheral blood. The results showed that curcumin treatment can significantly improve the severity of symptoms and delay the onset of EAE in mice and upregulate the AKT/mTOR autophagy pathway, resulting in low expression of the related proteins p-AKT, p-mTOR and p62; in contrast, the expression of LC3-II and Beclin 1 was significantly increased. In addition, the expression levels of soluble IFN-γ, IL-17 and TNF-α in the peripheral blood increased significantly in the EAE model group, while curcumin treatment significantly reduced the expression of these three inflammatory factors. Based on the above results, we have drawn the following conclusions. 1. Autophagy is closely related to the pathogenesis of EAE, and autophagy defects can lead to EAE-induced neuronal damage. 2. The AKT/mTOR signalling pathway is critical for autophagy regulation in EAE mice. 3. The therapeutic effect of curcumin on EAE mice may be mediated by the AKT/mTOR signalling pathway to upregulate the level of autophagy, while the expression levels of inflammatory factors, such as IFN-γ, IL-17 and TNF-α, in the peripheral blood were downregulated, which achieved a balance between autophagy and inflammation. Curcumin can successfully induce autophagy by regulating the AKT/mTOR signalling pathway with precise therapeutic effects, which provides an experimental basis for the identification of new drugs for the treatment of MS.

Funding

Financial support was received from 1.Gansu Provincial Department of Science and Technology of China (No. 1604WKCA015); 2. Province International Science and Technology Cooperation Base for Precise Treatment of Neurological Diseases;3. Research Discipline of Lanzhou University.

Role of the funding source

Financial support only.

Declaration of Competing Interest

None.

Acknowledgements

We would like to thank the teachers at the Animal Experimental Center of Gansu University of Traditional Chinese Medicine and the Basic Medical College of Lanzhou University for expert technical assistance.

References

Boland, B., Nixon, R.A., 2006. Neuronal macroautophagy: from development to degeneration. Mol. Asp. Med. 27, 503–519.

Bravo, B., Gallego, M.I., Flores, A.I., Bornstein, R., Puente-Bedia, A., Hernandez, J., de la Torre, P., Garcia-Zaragoza, E., Perez-Tavarez, R., Grande, J., Ballester, A., Ballester, S., 2016. Restrained Th17 response and myeloid cell infiltration into the central nervous system by human decidua-derived mesenchymal stem cells during experimental autoimmune encephalomyelitis. Stem Cell Res Ther 7, 43.

Chen, L., Xu, B., Liu, L., Liu, C., Luo, Y., Chen, X., Barzegar, M., Chung, J., Huang, S., 2015. Both mTORC1 and mTORC2 are involved in the regulation of cell adhesion. Oncotarget 6, 7136–7150.

Chi, B.H., Kim, S.J., Seo, H.K., Seo, H.H., Lee, S.J., Kwon, J.K., Lee, T.J., Chang, I.H., 2015. P70S6K and Elf4E dual inhibition is essential to control bladder tumor growth and progression in orthotopic mouse non-muscle invasive bladder tumor model. J. Korean Med. Sci. 30, 308–316.

Dendrou, C.A., Fugger, L., 2017. Immunomodulation in multiple sclerosis: promises and pitfalls. Curr. Opin. Immunol. 49, 37–43.

Evans, E., Piccio, L., Cross, A.H., 2018. Use of vitamins and dietary supplements by patients with multiple sclerosis: a review. JAMA Neurol. 75, 1013–1021.

Feng, J., Tao, T., Yan, W., Chen, C.S., Qin, X., 2014. Curcumin inhibits mitochondrial injury and apoptosis from the early stage in EAE mice. Oxidative Med. Cell. Longev. 2014, 728751.

Feng, X., Hou, H., Zou, Y., Guo, L., 2017. Defective autophagy is associated with neuronal injury in a mouse model of multiple sclerosis. Bosn. J. Basic Med. Sci. 17, 95–103.

Hemmer, B., Kerschensteiner, M., Korn, T., 2015. Role of the innate and adaptive immune responses in the course of multiple sclerosis. Lancet Neurol. 14, 406–419.

Hubbard, P.A., Moody, C.L., Murali, R., 2014. Allosteric modulation of Ras and the PI3K/AKT/mTOR pathway: emerging therapeutic opportunities. Front. Physiol. 5, 478.
Kabeya, Y., Mizushima, N., Ueno, T., Yamamoto, A., Kirisako, T., Noda, T., Kominami, E., Ohsumi, Y., Yoshimori, T., 2000. LC3, a mammalian homologue of yeast Apg8p, is localized in autophagosome membranes after processing. EMBO J. 19, 5720–5728.
Kanakasabai, S., Casalini, E., Walline, C.C., Mo, C., Chearwae, W., Bright, J.J., 2012. Differential regulation of CD4(+) T helper cell responses by curcumin in experimental autoimmune encephalomyelitis. J. Nutr. Biochem. 23, 1498–1507.
Kumar, S., Patel, R., Moore, S., Crawford, D.K., Suwanna, N., Mangiardi, M., Tiwari-Woodruff, S.K., 2013. Estrogen receptor beta ligand therapy activates PI3K/Akt/mTOR signaling in oligodendrocytes and promotes remyelination in a mouse model of multiple sclerosis. Neurobiol. Dis. 56, 131–144.
Ledinek, A.H., Sajko, M.C., Rot, U., 2013. Evaluating the effects of amantadin, modafinil and acetyl-L-carnitine on fatigue in multiple sclerosis–result of a pilot randomized, blind study. Clin. Neurol. Neurosurg. 115 (Suppl. 1), S86–S89.
Li, Z., Chen, L., Niu, X., Liu, J., Ping, M., Li, R., Xie, X., Guo, L., 2012. Immunomodulatory synergy by combining atorvastatin and rapamycin in the treatment of experimental autoimmune encephalomyelitis (EAE). J. Neuroimmunol. 250, 9–17.
Liang, P., Le, W., 2015. Role of autophagy in the pathogenesis of multiple sclerosis. Neurosci. Bull. 31, 435–444.
Lin, J., Huo, X., Liu, X., 2017. (mTOR signaling pathway): a potential target of curcumin in the treatment of spinal cord injury. Biomed. Res. Int. 2017, 1634801.
Mohajeri, M., Sadeghizadeh, M., Najafi, F., Javan, M., 2015. Polymerized nano-curcumin attenuates neurological symptoms in EAE model of multiple sclerosis through down regulation of inflammatory and oxidative processes and enhancing neuroprotection and myelin repair. Neuropharmacology 99, 156–167.
Orrenius, S., Kaminskyy, V.O., Zhivotovsky, B., 2013. Autophagy in toxicology: cause or consequence? Annu. Rev. Pharmacol. Toxicol. 53, 275–297.
Patergnani, S., Castellazzi, M., Bonora, M., Marchi, S., Casetta, I., Pugliatti, M., Giorgi, C., Granieri, E., Pinton, P., 2018. Autophagy and mitophagy elements are increased in body fluids of multiple sclerosis-affected individuals. J. Neurol. Neurosurg. Psychiatry 89, 439–441.
Schmid, D., Pypaert, M., Munz, C., 2007. Antigen-loading compartments for major histocompatibility complex class II molecules continuously receive input from autophagosomes. Immunity 26, 79–92.
Shen, X., Wang, M., Bi, X., Zhang, J., Wen, S., Fu, G., Xia, L., 2016. Resveratrol prevents endothelial progenitor cells from senescence and reduces the oxidative reaction via PPARgamma/HO1 pathways. Mol. Med. Rep. 14, 5528–5534.
Tian, F., Morimoto, N., Liu, W., Ohta, Y., Deguchi, K., Miyazaki, K., Abe, K., 2011. *In vivo* optical imaging of motor neuron autophagy in a mouse model of amyotrophic lateral sclerosis. Autophagy 7, 985–992.
Wei, Y., Gao, J., Qin, L., Xu, Y., Shi, H., Qu, L., Liu, Y., Xu, T., Liu, T., 2017. Curcumin suppresses AGEs induced apoptosis in tubular epithelial cells via protective autophagy. Exp. Ther. Med. 14, 6052–6058.
Wu, D.J., Adamopoulos, I.E., 2017. Autophagy and autoimmunity. Clin. Immunol. 176, 55–62.
Zhang, J., 2015. Teaching the basics of autophagy and mitophagy to redox biologists–mechanisms and experimental approaches. Redox Biol. 4, 242–259.
Zhen, C., Feng, X., Li, Z., Wang, Y., Li, B., Li, L., Quan, M., Wang, G., Guo, L., 2015. Suppression of murine experimental autoimmune encephalomyelitis development by 1,25-dihydroxyvitamin D3 with autophagy modulation. J. Neuroimmunol. 280, 1–7.